The impact of flexible environmental policy on maritime supply chain resilience

Zavitsas, Konstantinos; Zis, Thalis; Bell, Michael G.H.

Published in:
Transport Policy

Link to article, DOI:
10.1016/j.tranpol.2018.09.020

Publication date:
2018

Document Version
Peer reviewed version

The impact of flexible environmental policy on maritime supply chain resilience

This is a pre-print of an article published in

Transport Policy

The definitive publisher-authenticated version is available here:
https://www.sciencedirect.com/science/article/pii/S0967070X17303050

Zavitsas, K., Zis, T., & Bell, M. G. (2018). The impact of flexible environmental policy on maritime supply chain resilience. *Transport Policy*, *72*, 116-128.
https://doi.org/10.1016/j.tranpol.2018.09.020

The impact of flexible environmental policy on maritime supply chain resilience

Abstract

As policy makers acknowledge the high degree of supply chain vulnerability and the impact of coastal maritime emissions to coastal population health, there has been a consistent effort to strengthen maritime security and environmental regulations. In recent years, supply chain hyper-optimization has led to lean and tightly integrated systems with little additional buffers and high sensitivity to disruptions.

This study considers the designation of Emission Control Areas and establishes a link between environmental and network resilience performance for maritime supply chains using operational cost and SO_x emissions cost metrics. The proposed methodological framework analyzes various abatement options, disruption intensities, fuel pricing instances and regulatory strategies (such as the flexible implementation of ECAs). The methodology utilizes a minimum cost flow assignment and a link velocity optimization model for vessel speed to establish the payoff for various network states. Additionally, an attacker defender game is set up to identify optimal regulatory strategies under various disruption scenarios.

The results are complemented by a sensitivity analysis on SO_x emissions pricing, to better equip policy makers to manage environmental and resilience legislation. The methodology and findings provide a comprehensive analytic approach to optimize maritime supply chain performance beyond minimisation of operational costs, to also minimize exposure to costly supply chain disruptions.

Keywords: Network resilience, Supply chain management, Emission Control Areas, Attacker-defender game

1. Introduction

Maritime transportation has a major role in driving economic growth and globalization, as it accounts for four fifths of the world's total merchandise trade (UNCTAD, 2017). Since 1990,

the international merchandise trade volume has been growing twice as fast as the global economic growth (WTO, 2016). The excess trade growth may be associated with globalized production, increased trade in parts and components, greater economic integration, and deeper and wider global supply chains (Berle, 2011). As recognized in the Global Risk Report by the World Economic Forum (2016), the increasingly high degree of coupling and interaction between sources, stakeholders and processes together with the over-dependence on deeper, wider global chains, has made the operation of the international maritime network more susceptible to disruptions.

To address this challenge, since the early 2000s, there has been a consistent effort to strengthen maritime security through the introduction of several new regulations at global, regional, and national levels. Most notably these include, the International Ship and Port Facility Security (ISPS) code, other amendments to the International Safety of Life at Sea (SOLAS) Convention of 1974, the revised Seafarers' Identity Documents (SID) Convention of 2003, the Container Security Initiative, the 24-hour manifest rule and plans to introduce a global system for the long-range identification and tracking (LRIT) of ships. Raymond and Morrien (Lloyd's MIU, 2008) recognize that maritime security legislation amendments introduced since 2000 are primarily targeted to deal with terrorism threats and have limited impact against other types of disruptions. Furthermore, several studies discuss the practical implementation of security regulations, criticizing their impractical and overlapping nature, and the lack of a unified framework (Acciaro and Sierra, 2013; Bichou, 2008). Berle et al. (2011) recognize that:

- Practitioners have an operational (rather than strategic focus), therefore, their efforts focus on frequent minor disruptions rather than larger accidental events
- There is awareness that larger events do happen, and know that these are very costly, yet they do not prepare systematically to restore the system.

Evidence of costly "non-terrorism" related disruptions associated with the lack of a holistic security framework are frequently documented in supply chain resilience literature. From an international supply chain perspective, disruptions are found capable of severe and long-lasting impact, even when originating at remote locations very "deep in the supply network" (Hendricks and Singhal, 2005; Supply Chain Digest, 2006). Policies for addressing occasional high impact threats (e.g. political disputes and natural disasters) exist mainly at an industry specific context. For example, the International Energy Agency's (IEA) member countries are required to hold oil stock reserve equivalent to a minimum of ninety days of their net imports (IEA, 2007; IEA, 2014). In such cases, resilience is added through introducing slack. Most industries though do not have such policies in place. At the same time, supply chain hyper-optimization leads to lean and tightly integrated systems with little additional buffers and high sensitivity to disruptions.

Over-dependence on deeper and wider multinational supply and production chains also has environmental implications. The UNCTAD (2017) reported that if seaborne trade continues to grow at its current pace and no global action is taken to reduce CO_2 emissions in the sector, maritime trade and related CO_2 emissions would double by 2035. In 2011, the IMO introduced a set of global technical and operational measures to control CO_2 emissions from international shipping, such as the Energy Efficiency Design Index (EEDI) and the Ship Energy Efficiency Management Plan (SEEMP), that improve energy efficiency and reduce emissions intensity (CO_2/tonne-mile).

While the low CO_2 emissions figure enhances the argument that maritime shipping is the greenest mode of transport, shipping has a more significant contribution to other types of

emission pollutants. The sector is responsible for 5-8% of the global SO_2 emissions (Eyring et al., 2005), and approximately 15% for NO_x (Corbett et al., 2007). At the same time, about 60 thousand deaths related to respiratory health issues near coastlines are correlated to PM emissions from shipping. In response, the revised MARPOL Annex VI introduced limits on the maximum sulphur content allowed in bunker oil used by ships. This regulation also designated Emission Control Areas (ECA) where tighter limits applied. The limits on allowed sulphur content will become progressively stricter over the years for activity within and outside the ECA as shown in Table 1.

MARPOL designated the Baltic Sea as the first ECA for SO_x emissions in 1997 and enforced it after 2005, while the following year the North Sea was also designated as an ECA. Two newer ECAs include the North American ECA that extends 200 nautical miles (NM) from the coasts of North America and the US Caribbean Sea ECA, both of which target PM and NO_x emissions by setting a maximum limit of NO_x emissions per kWh used on-board. The regulation suggests that from 2020 onwards, the global limit of sulphur content will be 0.5% (outside ECAs) as shown in Table 1.

Table 1: Maximum allowed sulphur content (%)

	Year			
Areas	*2005-2012*	*2012-2015*	*2015-2020*	*2020-*
Within ECA	1.5	1	0.1	0.1
Outside ECA	4.5	3.5	3.5	0.5

Cullinane and Bergqvist (2014) encourage the further designation of ECAs due to the various socio-economic benefits these bring. However, such regulation increases the operating costs for the ship operators as more expensive fuel is required for compliance, or technological investments that ensure a similar reduction of SO_x emissions. M. Tichavska et. al. (2017) propose emission inventories built from AIS vessel tracks to provide policy making support in reducing the local and global impact of vessel emissions. Zis and Psaraftis (2017) developed a modal choice model to estimate the implications of ECAs on the short-sea shipping sector. They showed that modal shifts to land-based modes can be expected should bunker oil prices pick up again.

Sulphur content in vessel fuel legislation has been in place in the European Union with the 2005/33/EC directive that allows only the use of fuel with less than 0.1% sulphur from ships at berth in EU ports or when sailing through inland waterways. The use of low sulphur fuel is also enforced at a regional level, as for example in California, where from 2012 onwards ocean-going vessels are required to use 0.1% fuel within 24 NM from the Californian Coast (CARB, 2012), and by some port authorities that provide incentives for the use of low sulphur fuel in their proximity.

The aim of this research is to model the impacts of ECAs on maritime operations at sea, and associate them with network resilience performance indicators. Establishing this relationship will better equip policy makers to manage environmental and resilience legislation, and supply chain operators who consistently seek to minimise operational costs, also minimize their exposure to costly supply chain disruptions.

The following Section provides basic definitions and a methodological background for vessel emission modelling, describing the relationship between vessel speed, fuel consumption and

emissions that is key to linking and quantifying emissions regulations impact to maritime network resilience. In Section 3, the integrated modelling approach adopted in this work is presented and in Section 4 a case study is presented where the proposed modelling framework is applied in the context of the oil supply chain, followed by a discussion of findings. In the final section conclusions are drawn and suggestions for future research are made.

2. Methodological background

2.1. Vessel emission modelling

To comply with the low sulphur requirements of previous regulations, ship operators can either use low sulphur fuel such as Marine Gas Oil (MGO) or invest in newer technologies. One option is to equip vessels with scrubber systems that allow operators to use Heavy Fuel Oil (HFO), or alternatively invest in dual-fuel engines that permit the use of Liquefied Natural Gas (LNG). For vessels at berth, an additional option that secures compliance with most regulations is the use of 'cold ironing' where a vessel receives shore power from the grid (Zis et al., 2014). All options available to ensure compliance with regulations increase either the capital (technological investments) or operating (use of more expensive fuel) costs of running a vessel. As a result, the ECAs are anticipated to affect the profitability of a shipping service.

Fuel consumption depends on the fuel efficiency of machinery on-board at its current operating levels. Many studies attempt to model fuel consumption at a macroscopic level and do so using bottom-up activity methodologies (Psaraftis and Kontovas, 2012; Cariou, 2010; Corbett et al., 2009). A common finding in these studies is that the most significant fuel consumption component is during the cruise stage.

For modelling fuel consumption, three main activity modes that require energy are assumed for all ships; sailing (*S*), manoeuvring (*M*), and berth hoteling (*B*). For the majority of commercial vessels, there are dedicated engines on board that provide the necessary power for each activity phase. During sailing, the main engines (*m*) are operating to propel the vessel, while at the same time auxiliary engines (α) are running to cover the vessel's electricity demands (heating, lighting, refrigerating, pumps etc.). In some vessels, the energy for activities other than propulsion may be taken from the main engines when a shaft generator is used (Prousalidis et al., 2005). While the ship is manoeuvring to approach and depart from a port, the main engines are usually switched off and the auxiliary engines are running on higher loads to provide redundancy. Large vessels may require the assistance of tugboats during this activity phase, while at some ports a pilot must board the vessel at a certain distance from the port to lead the manoeuvring operation. Finally, when the vessel is at berth the auxiliary engines are operating to cover the electric demands of the vessel, and normally the main engines are switched off for long berth durations (typically 4 hours and above). Another type of machinery that contributes to the overall fuel consumption of a port to port journey is the auxiliary boilers (*b)* which are used whenever the main engines are switched off, and are responsible to maintain the fuel and main engine cylinder temperatures at the desired levels (Zis et al, 2014). The fuel consumption $FC_{i,A,k}$ (kg) for machinery of type *e*, on-board vessel *k*, during activity *A* is given by equation 1:

$$FC_{e,A,k} = 10^{-3} \cdot SFOC_{e,A,k} \cdot EL_{e,A,k} \cdot EP_{e,k} \cdot t_{A,k} \; with \; e \in E = \{m, a, b\}., A \in \{S, M, B\} \quad (1)$$

where:
$SFOC_{e,A,k}$ denotes the specific fuel oil consumption for the engine (g of fuel per kWh),

$EL_{e,A,k}$ (%) is the engine load expressed as percentage of the maximum continuous rating (MCR) of the engine,
$EP_{e,k}$ (kW) is the nominal engine power installed
and $t_{A,k}$ (hours) is the duration of the engine's activity.

Summing over the fuel consumption of each type of machinery operating during the different activities, will lead to the estimation of the fuel consumption per voyage. The engine loads for the auxiliary engines and boilers vary significantly from 10% to 60% (Khersonsky et al, 2007) and depend on the trip, cargo type, port, and weather. The most fuel demanding activity is sailing, where the load of the propulsion engines may reach 70% to 90%, depending on the sailing speed chosen. In the past, most engines were designed to have their optimal efficiency at 70-85% of MCR, however in recent years with the re-emergence of slow steaming the engines may run as low as 30% of MCR with even lower values suggested for super slow steaming instances (Maloni et al., 2013). This considerable change is attributed to the dependence of required output power with sailing speed. Most studies in the literature have been using the propeller law, which assumes an exponential relationship between engine load (EL) and sailing speed (V) . For example, the engine loads $EL_{m,S1,k}$ and $EL_{m,S2,k}$of the main engine m of vessel k at two different sailing speeds V_{S1} ad V_{S2} are linked as follows in equation 2 where *n* is the exponent used:

$$\frac{EL_{m,S1,k}}{EL_{m,S2,k}} = \left(\frac{V_{S1}}{V_{S2}}\right)^n \quad (2)$$

As a rule of thumb, *n* takes a value of 3, and therefore a cubic relationship applies (Ronen, 1982). For increased accuracy, a higher exponent is suggested for faster sailing speeds, and specific ship types, reaching a value of 4.5-5 for fast containerships (Psaraftis and Kontovas, 2013).
The propeller law explains why sailing at lower speeds has been occurring in recent years with the higher fuel prices. The optimal sailing speed problem was first defined on the basis of trade-offs between lower fuel costs and loss of vessel revenues associated with lower speeds (Ronen, 1982). This practice, commonly known as slow steaming, mitigates fuel costs during crises or when excess capacity exists in the shipping market (Benford, 1981). There are additional environmental benefits due to slow steaming, and it has been shown that despite an increase in the number of trips to meet the supply required, the lower sailing speed results in emissions savings (Cariou, 2010). Considering an individual tanker vessel that carries a main engine of 32000 kW and auxiliary power of 4500kW (very large crude carrier – VLCC), the fuel consumption per NM travelled for each type of machinery during cruise is depicted in Figure 1 (left y-axis).

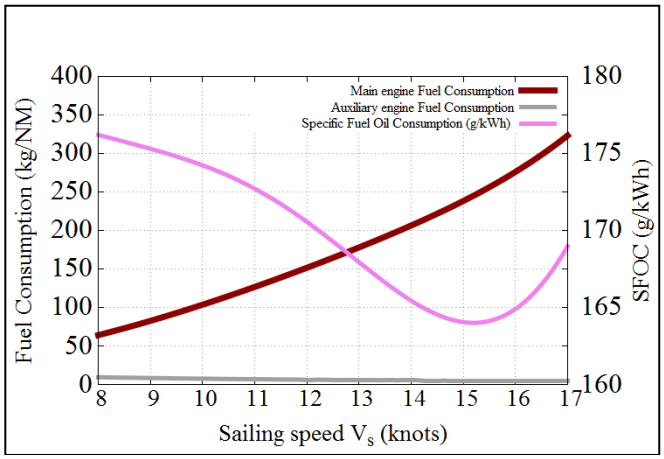

Figure 1: Fuel consumption per NM and SFOC variation at different sailing speeds (Data source: Man Diesel (2012)

The graph also shows the variation of SFOC (right y-axis) at the different speeds, which is shown to be suboptimal at lower loads. Despite the lesser efficiency, the fuel consumption is reducing at lower sailing speeds due to the less demand for power. Figure 1 also shows that the fuel consumption per NM for the auxiliary engine (grey line) is increasing at lower speeds, which is justified from the assumption that the energy requirements on-board are not depending on speed. Using equations 1 and 2 a connection between fuel consumption, vessel energy efficiency and vessel speed during various voyage activity modes is established that indicates vessel configuration under various service speeds. This enables the environmental performance of the network to be determined in periods of low and high demand and for any environmental legislation, which affects the selected operating profile of the engines.

2.2. Models for maritime supply chain resilience

The visibility of individual businesses along the operations of a supply chain tends to be limited to two or three chain links (Vilko and Hallikas, 2012). At the same time the fragmentation of supply processes and increasing chain depth, reduce further that visibility threshold, and when a disruption occurs beyond it, little can be done by unprepared individual stakeholders to withhold it. Although, production economics literature has highlighted the importance of information exchange with supply chain partners, Lai et. al. (2015) illustrate that there are limited cost benefits by exchanging environmental management information.

Studies focusing on the shipping aspect of supply chain vulnerability have relied mostly on complex network models, which can be classified as either pure-topological or flow-based models (Ouyang et. al., 2014; Lhomme, 2015; Cox et. al., 2011; Reggiani, 2013). The majority of pure-topological models assess disrupted network performance using metrics such as network density, average degree, centrality of components, maximum and minimum distances, connectivity, correlation, and clustering (Wasserman and Faust, 1994; Duceret and Zaidi, 2012). Kim et al (2015) use a pure-topological approach and define disruptions at arc-, node- and network- level, to establish that for networks of unweighted links, scale free supply structures offer better resilience. Pure-topological models adopt binary network representations (e.g. link available or not) to rank critical components (Angeloudis, et. al., 2007; Duceret, et. al., 2010). Furthermore, Sullivan et al. (2010) argue that the main problem of pure-topological models is the creation of isolated sub-networks that are inaccessible after component removal. Such approach cannot be applied to evaluate the impact of disruptions on network capacity, travel times or processing times (Qiao, et. al., 2014), nor to quantify any costs of cargo rerouting. These limitations can severely restrict studies on maritime supply chain operations, where partial disruptions are more frequent than complete failures and, isolated subnetworks

are less likely in maritime supply chains operations, as vessels and cargoes can be rerouted. In contrast, flow-based models use costs, operational and physical constraints, to capture the redistribution of commodity flows subject to capacity limitations, integral to existing network configurations[1].

Sheffi and Rice (2005) who examine supply chain resilience from an enterprise perspective, suggest that resilience can be achieved by either creating redundancy or increasing flexibility. While redundancy is part of every resilience strategy, it represents sheer cost with limited benefit unless when a network is disrupted. Focusing on maritime operations, fleet operational capacity is defined as a function of deadweight tonnage and vessel speed. It can therefore be increased, either by shipbuilding or increasing vessel speed. With increasing vessel speed being the only viable short-term measure, Zavitsas (2011) argues that the concept is reverse to slow steaming. When slow-steaming takes place, maritime operations have high redundancy, which can be utilised instantly by increasing vessel speed offering resilience to the network.

2.3. Linking environmental policy to network resilience performance

In maritime supply chain operations, when an optimal maritime link is disrupted, flow is rerouted to a less optimal, typically longer route. Assuming that vessel speed remains the same, the travel time to serve the same origin destination route will increase, and round-trip frequency will reduce. A link disruption influences all vessels whose route goes through that link. The total disruption impact is, therefore, proportional to the carrying capacity of the fleet influenced and the delay the rerouting causes.

As shown by equation 2 fuel consumption and vessel emissions are directly linked to vessel speed too. A link can therefore be made between maritime fleet speed to maritime supply chain capacity redundancy, and environmental emissions. The relationship presented in Figure 2 is a bi-directional one as when one component changes all others increase or decrease as well. As discussed in Section 2.2, in the long term, shipbuilding capability can also assist in overcoming the impact of a link disruption. Although, this research focuses on short-term response, the long-term cycle is also illustrated in Figure 2. To capture adjacent components (linked by an arrow ‘‘→’’) type of association in Figure 2, the symbol ‘‘+’’ after a variable is used to indicate a concurrent relationship with the following variable of the chain, while the symbol ‘‘−’’ implies an opposite relationship. The components illustrated in Figure 2 are applicable both at individual vessel and maritime fleet levels.

Short-term cycle: Emissions $\overrightarrow{+}$ Fuel consumption $\overrightarrow{+}$ Average speed $\overrightarrow{+}$ Operational capacity $\overrightarrow{+}$ Level of redundancy $\overrightarrow{+}$ Resilience

Long-term cycle: Operational capacity $\rightrightarrows$ Shipbuilding $\overrightarrow{+}$ Fleet tonnage $\overrightarrow{+}$ Operational capacity

The short-term cycle describes the instantaneous changes in environmental performance and resilience respectively (shown in continuous line links in Figure 2). The long-term cycle can be expressed in the following way: “Operational capacity deficit will yield shipbuilding to scrapping ratio > 1, which will yield higher fleet tonnage”.

[1] The reader is referred to Levalle and Nof (2014), Perea et al. (2015) and Achurra-Gonzalez, et.al. (2016) for a more detailed literature review and discussion on flow-based approaches for supply chain resilience assessment.

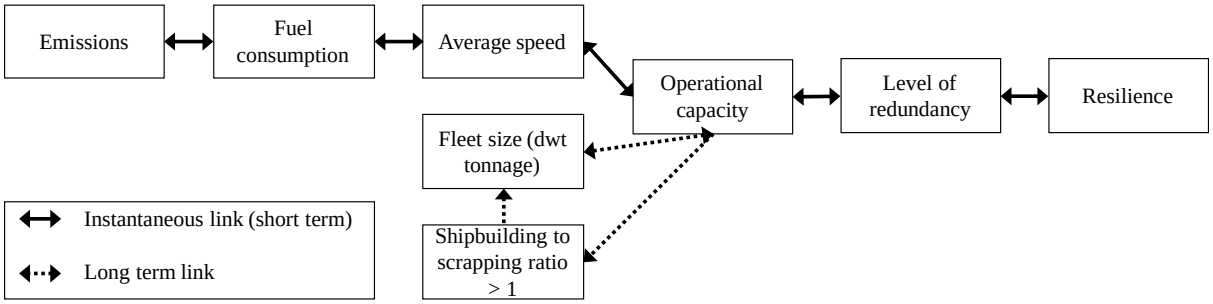

Figure 2: Short- and long-term associations to changes in maritime fleet speed

This research assumes that the stricter environmental regulations (such as the introduction of ECAs) can be handled by ship operators through a reduction of average vessel speed as a coping mechanism. Recent research suggests that only ship operators that sail almost exclusively within ECAs may invest in scrubber retrofits (Zis and Psaraftis, 2018). In this paper, within the examined networks the tanker fleet is only spending 13% of their time within ECAs, and therefore we can safely assume that ship operators will use fuel switching to comply with the regulation. Therefore, the sulphur content restriction is expected to assimilate the effects observed in slow steaming instances to some extent due to the overall higher operating costs stemming from the regulation leading to a lower optimal sailing speed. The modelling framework proposed in this research consists of a minimum cost flow assignment model (MCFAM), a supply chain resilience game model (SCRGM) using game theory attacker-defender models to capture legislative and disruption choices and a link velocity optimization model (LVOM). The framework captures the operational expenses and SO_x emissions cost for various disruption scenarios and regulatory frameworks, and it is used to consider a flexible approach in the implementation of environmental policy.

3. Modelling framework

The modelling framework proposed in this research integrates the MCFAM, SCRGM and LVOM to form two separate loops as illustrated in Figure 3, aligned so that one model's output feeds to another model as input. A macroscopic modelling approach is adopted in this research, to maintain tractability of the model even in large scale network applications that supply chains typically are.

Table 2: MCFAM, SCRGM and LVOM notation

Sets		**Indices**	
A	All arcs	i	Starting node
V	All nodes	j	Ending node
L	Land transport modes	m	Mode of transport
W	Maritime transport modes	q	Commodity
R	All regions within a link	k	Intermediate node
E	All machinery on board	r	Region within link (ECA/ No ECA)
Π	Payoff matrix	e	Engine type (main/ aux./ boiler)
S_n	Conductor mixed strategies	σ	Conductor pure strategies
S_m	Disruptor mixed strategies	κ	Disruptor pure strategies
Parameters			
$d_{i,j,m}$	Arc (i,j)distance when mode m is used		
$c_{i,j,m,q}$	Unit cost when commodity q flows in arc (i,j) using mode m		
$u_{i,j}$	Shared arc capacity for all land transport modes $m \in L$ when arc (i,j) is fully operational		
$u'_{i,j}$	Disrupted arc capacity		
$u_{m,q}$	Fleet capacity for all maritime transport modes $m \in W$		
EL	Vessel engine energy level		
u_k	Capacity of processing facility		
$S\%$	Percentage of sulphur content in fuel		
D_r	Length of region r in NM		
P_r	Price of fuel in region r in \$/tonne		
EP_e	Nominal installed power of engine e		
Decision variables			
$f_{i,j,m,q}$	Flow of commodity q assigned to arc(i,j) using mode m		
$z_{\overline{EL}}$	Uniform factor on maritime fleet EL		
V_r	Sailing speed in region r		
X^*	Conductor optimal mixed strategy decision vector		
Y^*	Disruptor optimal mixed strategy decision vector		
Auxiliary variables			
EL	Engine load as % MCR		
$z_{\overline{EL}}$	Uniform factor on maritime fleet EL		
$SFOC_e$	Specific fuel oil consumption of engine e in g/kWh		
$\overline{V}_{m,q}$	Universal fleet speed		
$a_{\sigma\kappa}$	Game payoff for conductor strategy σ and disruptor strategy κ		

3.1. Minimum cost flow assignment (MCFAM)

A minimum cost flow assignment model is used to capture the trade flows of a global supply chain network, and the rerouting that occurs when a component is disrupted. The formulation for the multi-origin, multi-destination, multi-mode and multi-commodity flow assignment assumes that every supply chain is modelled as a network of nodes V that represent ports, or processing facilities, and directed arcs A. Arcs are indicated by (i,j), listing a starting node i, and an ending node j. Arcs have a unique distance $d_{i,j}$, and a cost $c_{(i,j),m,q}$ applies when commodity $q \in Q$ and mode $m \in M$, flows in arc (i,j) that resembles fuel costs per trip. The set of modes M consists of land transport modes $m \in L$, and water transport modes $m \in W$, so that $M = L \cup W$. The decision variable $f_{(i,j),m,q}$ is the flow of commodity q assigned to arc (i,j) using mode m. Arc capacity is denoted by $u_{i,j}$ for all land transport modes $m \in L$ when arc is fully operational, while it is considered unlimited for water transport models $m \in W$. To account for the disruption game described in Section 3.3, disrupted arc capacity $u'_{i,j}$ is defined

for all modes $m \in M$. To account for fleet capacity on maritime links $m \in W$, $u_{m,q}$ is also defined. The demand of commodity q at each node $k \in V$ is defined to be $b_{k,q}$. The capacity of a processing facility at node $k \in V$ is defined as u_k. To solve this as a linear program, a heuristic approach is adopted for calculating and updating unit cost $c_{i,j,m,q}$ for maritime links $m \in W$. Initially, it is assumed that all vessels operate at slow steaming conditions using $EL = 40\%$. By using the propeller law shown in equation 2 this can be translated to a fleet sailing speed, fuel consumption that informs $c_{i,j,m,q}$ and vessel emissions. Then, the following minimum cost flow assignment problem can be solved:

$$\min_{f_{i,j,m,q}} \sum_q \sum_m \sum_{(i,j)\in A} c_{i,j,m,q} f_{i,j,m,q} \tag{3}$$

Subject to:

$$\sum_m \sum_i f_{(i,k),m,q} - \sum_m \sum_j f_{(k,j),m,q} = b_{k,q} \qquad \text{for all } k \in V, q \in Q \tag{4}$$

$$\sum_m \sum_q f_{(i,j),m,q} \leq u'_{i,j} \qquad \text{for all } (i,j) \in A, m \in L \tag{5}$$

$$\sum_m \sum_i \sum_q f_{i,j,m,q} \leq u_k \qquad \text{for all } k \in V \tag{6}$$

$$f_{i,j,m,q} \geq 0 \qquad \text{for all } q, m, (i,j) \in A \tag{7}$$

Constraint 4 ensures the conservation of flow at all network nodes, while constraint 5 ensures the capacity of land modes arcs is not exceeded. Constraint 6 ensures the throughput capacity of intermediate nodes is not exceeded, while constraint 7 ensures non-negative flows. Furthermore, the maritime travel demand for each commodity q should always be lower than the fleet capacity available as expressed by equation 8.

$$\sum_{(i,j)} f_{i,j,m,q} \leq u_{m,q} \qquad \text{for all } q \in Q, m \in W \tag{8}$$

Fleet capacity $u_{m,q}$ is a function of the average fleet speed $\overline{V}_{m,q}(EL)$ as described in Section 2.3. By expressing fleet capacity, as a function of engine load (EL) as shown in equation 9, the minimum EL to satisfy maritime travel demand can be determined.

$$u_{m,q} = dwt_{m,q} \times \overline{V}_{m,q}(EL) \qquad \text{for all } q \in Q, m \in W \tag{9}$$

As discussed in Section 2.1, EL is typically 70-85% at nominal sailing speed. In slow steaming conditions EL can go down to 30%. The proposed MCFAM assumes EL is common across the fleet, and if the EL value exceeds 100%, the problem is deemed unsolvable, as the fleet capacity redundancy is not sufficient to satisfy excess maritime travel demand. After obtaining the EL required to satisfy fleet capacity for each instance of the network examined (disrupted or not disrupted), a uniform factor $z_{\overline{EL}}$ is assumed so that:

$$\overline{EL}_{Instance} = z_{\overline{EL}} \times \overline{EL}_{SlowSteaming} \tag{10}$$

The maritime link costs $c_{i,j,m,q}$ are updated using the propeller law of equation 2 and the EL factor $z_{\overline{EL}}$ calculated by equation 10 to evaluate the updated network cost for satisfying all supply demand. By using the updated EL and average fleet speed $\overline{V}_{m,q}(EL)$, maritime fleet emissions are also determined. The total transport cost as determined by the MCFAM considers

maritime fleet and land modes (e.g. pipelines) operational costs and emissions cost. Route flows act as inputs to the SCRGM and LVOM models that compose the rest of the proposed methodological framework. In the current state of the model, sailing speed varies uniformly, however, the consequences of a universal fleet speed on port congestion are not considered. One approach that should be incorporated in the liner shipping network case, is the one in Golias et. al. (2014), that considers berth scheduling and minimizes port congestion.

The generation of harmful pollutant emissions can be easily estimated based on the fuel consumption of each vessel activity (sailing, manoeuvring, at-berth) and multiplying with an appropriate emissions factor. In this work, the focus is only on SO_x emissions as these are the targets of the ECA regulation. The generated emissions are found by multiplying the fuel consumption with *0.02 S%* where S% is the percentage of sulphur present in the fuel. In this work we assume that *S*=0.1 within ECAs (to comply with the regulation) and *S*=3.5 outside ECAs (the current maximum sulphur content allowed), while all auxiliary engines always use fuel with *S*=0.1. The benefit of the regulation is the reduced SOx emissions that may impact health of local population affected, lead to acid rain, and have various other environmental effects. To incorporate the benefit of reduced SOx emissions in our modelling framework, we consider the external costs associated with this pollutant.

The process of internalizing external costs is a policy measure that has been contemplated in the past, and there have been various studies attempting to identify the so called "damage costs" of various pollutants. As a baseline and starting point value, we consider the external cost of transport as 10.96$ per kg of SO_x emitted in sea areas as calculated in the handbook of estimation on external costs (Ricardo-AEA, 2014). This value is not paid by the polluter, but it can be used as a means to quantify the benefits of the regulation in environmental terms. It should be noted that during shipping activities there are other pollutants generated which also can be quantified in monetary terms using external costs. In addition, there are environmental trade-offs that must not be neglected; for instance, measures that reduce SO_x emissions have been proven to increase CO_2 emissions. However, in the context of this paper we only consider monetary values for sulphur emissions.

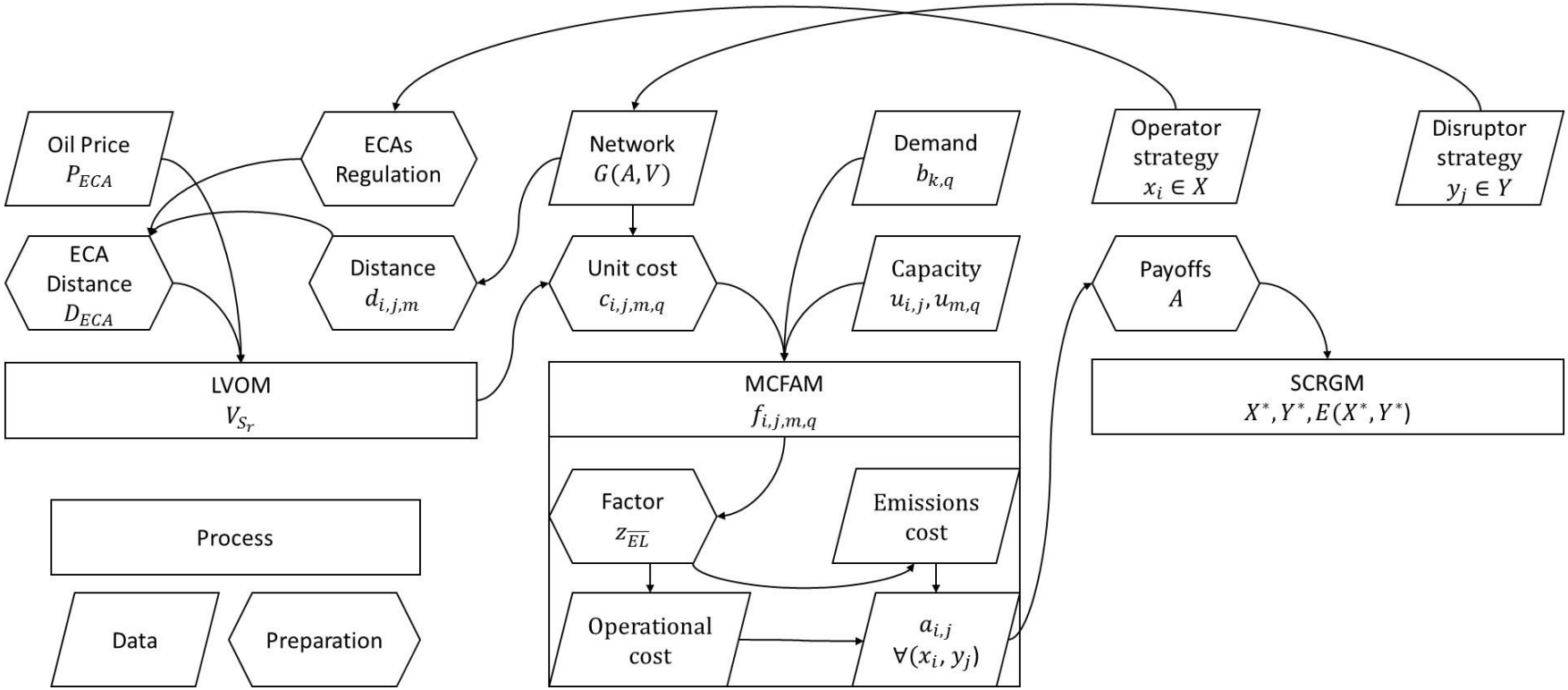

Figure 3: Performance assessment framework for eco-friendly and risk averse maritime network operation

3.2. Link velocity optimization model (LVOM)

Since the introduction of ECAs, the calculation of fuel cost has become more complex. For the links that contain legs within and outside ECAs, the vessel may have to switch fuel if it is not equipped with other abatement options (e.g. scrubber systems). In this case, an optimization problem can be formulated with the objective of minimizing total fuel costs within a specific link.

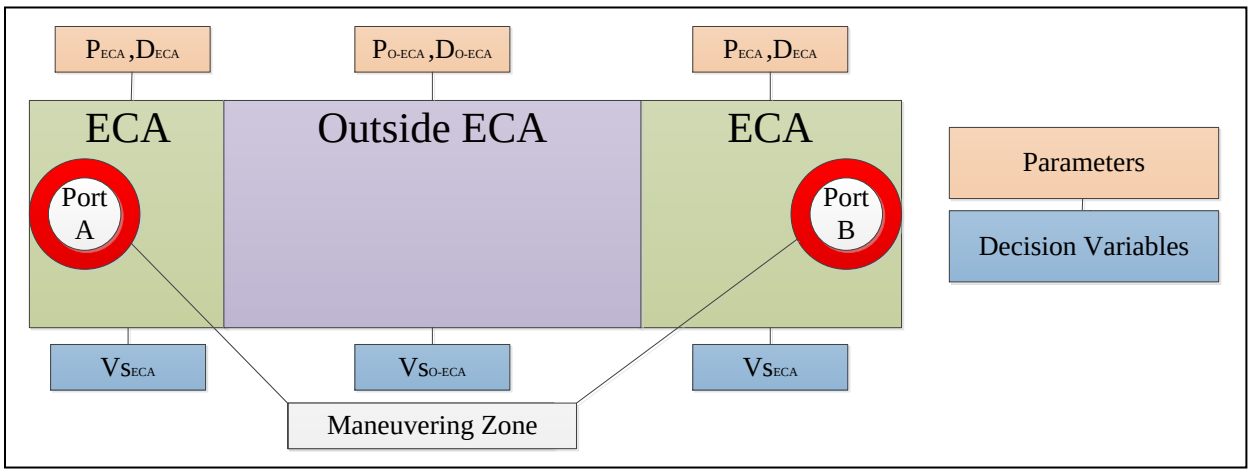

Figure 4: The speed differentiation problem

Figure 4 illustrates the speed differentiation problem where the decision variables are the sailing speed at each leg where a different fuel requirement applies. The main parameters of the problem are the fuel prices within an ECA (P_{ECA}) and outside ($P_{O\text{-}ECA}$) and the respective sailing distances (D_{ECA} and $D_{O\text{-}ECA}$). It should be noted that apart from speed differentiation, the ECA refraction problem has been proposed by Fagerholt and Psaraftis (2015), whereby the objective is to minimize the sailing distance within ECAs. The speed differentiation problem in the presence of ECA has been considered from an environmental perspective in previous studies (Doudnikoff et al., 2014) to show that there are increased CO_2 emissions, and in conjunction with speed limits near ports to illustrate that ECAs may complement such port authority initiatives (Zis et al., 2015). This research uses a simplified formulation of the latter study for each link *q* that consists of legs *r* of set *R*={ECA, O-ECA, ECA..} and considers the fuel consumption of each onboard machinery *e* of set *E* during sailing activity *S*.

$$\min_{V_r} \sum_{r\in R} \sum_{e\in E} P_r \cdot 10^{-6} \cdot \frac{D_r}{V_r} \cdot (EP_e \cdot EL_e \cdot SFOC_e) \tag{11}$$

Subject to:

$$V_r \leq V_{max} \qquad \text{for all } r \in R \tag{12}$$

$$V_r \geq 0 \qquad \text{for all } r \in R \tag{13}$$

$$\sum_{r\in R} \frac{D_r}{V_r} = \frac{\sum_{r\in R} D_r}{\overline{V}_{m,q}} \tag{14}$$

Constraint 12 ensures that the sailing speed at any leg cannot exceed the maximum allowed speed V_{max} for the vessel. Constraint 13 is a non-negativity constraint for the sailing speed. Constraint 14 ensures that the total sailing time at the link is the same as the original (e.g. without speed differentiation and sailing at all legs within a link with $\overline{V}_{m,q}$ as calculated from

the MCFAM model). The maximum sailing speed $V_{max}$of a vessel is assumed to be for MCR at 100 %. In reality, a vessel can sail at higher than 100 % MCR loads for limited periods of time during emergencies, but not more than 1 hour for each 12 hours of activity to avoid engine damage (Man Diesel, 2014). The proposed optimization problem is non-linear due to the power law dependency of the engine load to sailing speed. However, the objective function is convex monotonic and as a result, the problem can be easily solved with commercial solvers following linearization of the objective function. All other variables in the speed differentiation problem are taken from equation 1 in section 2.1.

3.3. Supply chain resilience game (SCRGM)

To establish what is the optimal operator and regulator strategy (assuming the two can act as a single entity), an attacked defender model is proposed. The game is set as a two-player, non-cooperative, constant sum, mixed strategy, complete information, instantaneous game. The integrated operator and regulator player, we call the "conductor", can choose out of three pure strategies: Strategy 1 is a baseline scenario, where the conductor operates the network minimizing operational cost and complying with ECA regulations. Strategy 2 is an enhanced operation scenario, where the conductor operates the network minimizing operational cost, complying with ECA regulations, and using the LVOM to do so in a reduced cost way. Strategy 3 resembles an emergency operation scenario, where the conductor operates the network minimizing operational cost and not complying with ECA regulations. The components of the three strategies available to the conductor are summarized in Table 3.

Table 3: Conductor set of strategies and each strategy's components

Conductor Strategy i	Minimize operational cost (MCFAM)	Comply with ECA regulations	Optimize link velocities (LVOM)
1	X	X	
2	X	X	X
3	X		

The disruptor strategies involve disrupting one of the network components (either of arcs A or nodes V). Although the proposed framework does not restrict the capabilities of the disruptor as to which one, it is noted that disruptions can be either complete or partial. For complete disruptions $u'_{i,j} = 0$, while for partial disruptions arc capacity is reduced so that $u'_{i,j} \leq u_{i,j}$. In a similar manner the analytic framework can also account for the disruption of fleet capacity $u_{m,q}$. To capture the resilience options for the conductor more vividly, the analysis assumes two intensity levels for the disruptor. Intensity 1 resembles disruptions as caused by Nature, where all disruptions have an equal likelihood and therefore delivering a sub-optimal. Intensity 2 resembles terrorist type disruptions, where the disruptor tries to maximize his payoff.

The payoff matrix $\Pi = (a_{\sigma\kappa})$, where σ and κ are the indexes for the conductor and disruptor pure strategies respectively, is populated using the MCFAM described in Section 3.1, and the LVOM described in Section 3.2. In this mixed strategy game, the probabilities of choice of each strategy represent time (or duration). For the disruptor this is associated to the likelihood of the network being in a specific state of disruption while for the conductor to the likelihood of the network being under a specific regulatory and operational state. The mixed strategy vector for the conductor is $X = (x_1, \dots, x_{n=3})$ where $X \in S_n$ and for the disruptor $Y = (y_1, \dots, y_m)$, where $Y \in S_m$. In mixed strategy games x_1 and y_1 represent the strategy choice

probabilities for each player respectively. As discussed there are three pure strategies available to the conductor, while m is equal to the number of disreputable network components. Then, the expected payoff of the game can be defined by:

$$E(X,Y) = \sum_{\sigma=1}^{3} \sum_{\kappa=1}^{n} x_\sigma a_{\sigma\kappa} y_\kappa = X\Pi Y^T \quad (15)$$

Using the above definitions, the supply chain resilience game formulation can be developed.

$$\max_{y_\kappa} \min_{x_\sigma} \sum_{\sigma=1}^{3} \sum_{\kappa=1}^{m} x_\sigma a_{\sigma\kappa} y_\kappa \quad (16)$$

Subject to:

$$\sum_{\sigma=1}^{3} x_\sigma = 1 \quad (17)$$

$$\sum_{\kappa=1}^{m} y_\kappa = 1 \quad (18)$$

$$x_\sigma, y_\kappa \geq 0 \qquad \text{for all } x_\sigma \in X, y_\kappa \in Y \quad (19)$$

Constraints 17 and 18 ensure that the total probability assigned to each players strategies does not exceed 100%, and constraint 19 ensures that no negative probabilities are assigned. The saddle point of the game of probability vectors $X^* \in S_3$ and $Y^* \in S_m$, is where equilibrium occurs so that the criterion illustrated in equation 20 is satisfied.

$$E(X,Y^*) \leq E(X^*,Y^*) \leq E(X^*,Y) \qquad \text{for all } X \in S_3, Y \in S_m \quad (20)$$

4. Case study

The methodological framework presented in Section 3 is applied to a simplified version of the global oil supply chain. The international oil supply chain, is a well-monitored network with sufficient availability of macroscopic data, such as international oil flows, exporting and importing regions, locations of processing facilities like refineries, maritime and land distances.

4.1. A miniature oil supply chain model

The miniature network set up for this case study is illustrated in Figure 5 and the data inputs used are summarized in Table 4 and Table 5 below.

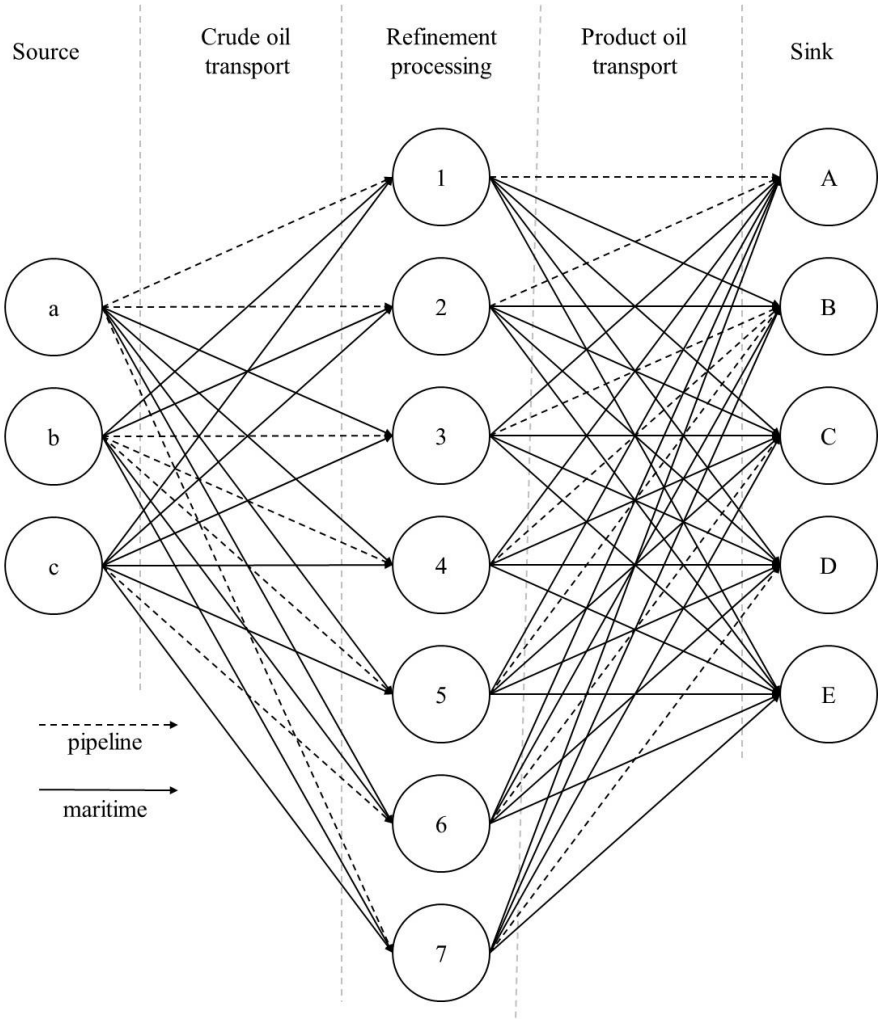

Figure 5: Miniature oil supply chain model with crude oil and oil products transport legs

The supply chain, consists of three source nodes, five sink nodes and seven intermediate processing nodes that represent oil refineries. The two commodities q transported are crude and product oil, and the modes m available for the transport legs are assumed to be only pipelines and maritime links as illustrated in Figure 5. The throughputs assumed for the source and sink node flows $b_{k,q}$, the distances between all nodes and the refineries capacity u_k are summarized in Table 4.

Table 4: Arc distances & ECA percentages in parenthesis (pipeline arcs underlined), refinery throughputs, source and sink node flows

	1	**2**	**3**	**4**	**5**	**6**	**7**	**b_k**
a/A	<u>5000</u>	<u>200</u>	11431 (22.7)	11503 (22.5)	17087 (34.7)	10038 (22.1)	2179	**a:** -9.87 **A:** 2.917
b/B	15937 (16.3)	11624 (22.3)	<u>200</u>	<u>100</u>	<u>2000</u>	13983 (5.3)	9923 (20.5)	**b:** -7.46/ **B:** 20.8
c/C	14528 (15.3)	10215 (21.8)	13967 (2.7)	14040 (2.6)	19207 (24.1)	<u>200</u>	8051 (13.8)	**c:** -11/ **C:** 2
D	6678 (100)	2414 (100)	9966 (22.3)	10039 (22.1)	15533 (33.4)	8110 (13.7)	<u>300</u>	2.518
E	13256 (8.38)	8993 (12.36)	12745 (2.91)	12817 (2.89)	17984 (19.6)	1656 (0)	6829 (21.7)	0.095
u_k	3	2	7	9	5	3	2.5	

In Table 5, the unit costs for all modes and commodities are presented for various vessel speeds. The capacity of pipeline arcs $u_{i,j}$ is assumed to be unlimited while vessels' and fleet capacities are obtained based on tanker fleet data (UNCTAD, 2017) on size, tonnage and classification. Although vessels vary in size, for the calculation of unit costs a representative standardized vessel type and size is assumed. For crude oil transport, the standard is assumed to be a 250000 dwt VLCC vessel; while for product oil transport the standard is a 70000 dwt Panamax Product tanker. Due to the small size of the modelled network and its sensitivity to sways of demand, it is assumed that the tanker fleet can be utilized both towards crude and product oil transportation.

Table 5: Arc unit costs (USD/ m bbl km) per vessel speed for average fuel pricing scenario (MGO: 700$/t, HFO: 400$/t)

m, q	**FUEL**	**SAILING SPEED (KNOTS)**									
		11	12	13	14	15	16	17	18	u_{mq}	u_{ij}
		$c_{i,j,m,q}$ **(USD/m bbl km)**									
VLCC (250000 DWT)	HFO	22	26	30	35	40	45	51	56	104	
	MGO	39	46	53	61	69	79	88	99		
PANAMAX PRODUCT (70000 DWT)	HFO	26	30	34	39	44	49	55	62		
	MGO	45	52	59	68	77	86	97	108		
PIPELINE (crude & product)		10									∞

For maritime shipments, the unit cost per tonne-NM is assumed to be higher for product tankers due to typically smaller vessel size. The unit cost values illustrated in Table 5 are obtained assuming fuel prices (FP1) MGO: 700$/t and HFO: 400$/t. To account for the variation in fuel price, the analysis is repeated for a high fuel price scenario (FP2) that assumes MGO: 1025$/t and HFO: 650$/t, and a low fuel price scenario (FP3) that assumes MGO: 380$/t and HFO: 190$/t.

Each link's unit cost is measured for each route and scenario separately depending on the links length within ECA, where only MGO fuel can be used. The location of all nodes in the real world is only important for calculating the mileage each arc covers within an ECA zone. Therefore, it can be said that nodes "a" and "A" represent St. Petersburg of Russia, "b" and "B" represent Houston of United States of America, "c" and "C" represent Jeddah of Saudi Arabia, "D" represents Hamburg of Germany, and "E" Limassol of Cyprus. Refinery nodes "1" and "2" represent Angarsk and Kirishi refineries of Russia respectively, "3", "4" and "5" represent Port Arthur, Texas City, and Carson refineries of United States of America respectively, "6" represents Rabigh refinery of Saudi Arabia and "7" represents Wilhelmshaven refinery of Germany. The ECA percentages are illustrated in Table 4.

The results from the application of the link speed optimization model (LVOM) show that the fuel cost per trip is minimized with a significant speed differential between regulated and non-regulated waters. This differential increases for instances where the regulated leg is short in comparison to the full voyage distance. This can be attributed to the fact that there is a longer leg in which the vessel can speed up to maintain its schedule. Comparing the differences in fuel prices, it is observed that at lower prices there is greater variation in the speeds as the relative difference is higher (MGO 90% higher, whereas in 2014 it was 55% higher). However, it should be noted that the speed differentiation leads to increased fuel consumption overall, and therefore more CO_2 emissions are generated per trip, while within the ECA even lower

SO_2 emissions will be observed. Therefore, the designation of ECA brings environmental consequences by reducing sulphur emissions in two ways at a cost of higher carbon emissions, and also leads to negative economic implications to the ship operators.

Table 6: OpEx pyoffs for average fuel pricing scenario and universal fleet speed for all strategy ***i*** and ***j*** combinations

OpEx Payoff (Speed adjusted OpEx)				Universal fleet speed (knots)			
Disruptor strategy ***j***	Conductor strategy ***i***			Disruptor strategy ***j***	Conductor strategy ***i***		
	1: ECA	2: ECA_opt	3: ECA		1: ECA	2: ECA_opt	3: ECA
None	5.22	5.17	4.92	None	11.97	11.97	11.97
a1	6.18	6.11	5.75	a1	12.52	12.52	12.52
a2	5.41	5.36	5.12	a2	11.97	11.97	11.97
a7	7.05	6.95	6.47	a7	12.91	12.91	12.91
b4	5.24	5.19	4.94	b4	11.98	11.98	11.98
b5	7.36	7.26	6.61	b5	12.94	12.94	12.89
c6	8.76	8.68	8.31	c6	13.76	13.76	13.76
1A	6.18	6.11	5.74	1A	12.52	12.52	12.52
2A	5.41	5.36	5.12	2A	11.97	11.97	11.97
3B	31.18	27.91	28.24	3B	18.69	18.69	18.69
4B	65.7	33.89	59.02	4B	22.5	22.5	22.5
5B	15.73	15.5	14.2	5B	15.71	15.71	15.71
6C	9.23	9.15	8.75	6C	13.85	13.85	13.85
7D	6.3	6.24	5.83	7D	12.44	12.44	12.44
a4	5.22	5.17	4.93	a4	11.97	11.97	11.97
c3	5.24	5.19	4.94	c3	11.98	11.98	11.98
c4	6.13	6.05	5.58	c4	12.43	12.43	12.4
2D	5.22	5.17	4.93	2D	11.97	11.97	11.97
6E	5.34	5.29	5.04	6E	12.04	12.04	12.04
All other	5.22	5.17	4.92	All other	11.97	11.97	11.97

The fleet capacity for tankers (both product and crude oil), shown in Table 5 is obtained by running a baseline scenario that assumes there is no network disruption, the ECAs regulation is in place and, universal fleet speed is 12 knots. For the baseline scenario the total speed adjusted operational cost is found to be 5.22 m$ and, the SO_x emissions cost is 1.61 m$. The fleet capacity required to satisfy demand (assuming 12knots vessel speed) is 104 million dwt. By running the MCFAM and LVOM repeatedly using Excel Solver the payoff matrix illustrated in Table 6 is populated considering all disruptor and conductor strategies.

In this case study the disruptor is assumed capable to fully disrupt one network arc at a time. Node and partial disruptions are not considered. Out of the 56 disruption scenarios considered only for the 18 shown in Table 6, a change in payoff was observed. For all others the same payoff to the baseline scenario (no disruption) was observed and are grouped together under "all other". For disruption scenarios 3B and 4B, the average fleet vessel speed obtained exceeds the maximum feasible EL, and therefore represents disruptions that cannot be addressed solely by increasing vessel speed. Disruption scenarios 3B and 4B, cannot be captured accurately by this model and are therefore not considered further in the analysis.

The payoffs obtained for the high and low fuel pricing scenarios (FP2 and FP3) are illustrated in Table 11 and Table 12 in the Appendix section.

Table 7: SO_x emissions cost and total payoff for FP1 scenario for all strategy i and j combinations

SO_x Payoff within ECA (m$)				Total Payoff (m$)			
Disruptor strategy j	Conductor strategy i			Disruptor strategy j	Conductor strategy i		
	1: ECA	2: ECA_opt	3: ECA		1: ECA	2: ECA_opt	3: ECA
None	0	0	0.11	None	5.22	5.17	5.03
a1	0	0	0.14	a1	6.18	6.11	5.89
a2	0	0	0.11	a2	5.41	5.36	5.23
a7	0.01	0	0.2	a7	7.06	6.95	6.67
b4	0	0	0.11	b4	5.24	5.19	5.05
b5	0.01	0	0.17	b5	7.37	7.26	6.78
c6	0	0	0.14	c6	8.76	8.68	8.45
1A	0	0	0.14	1A	6.18	6.11	5.88
2A	0	0	0.11	2A	5.41	5.36	5.23
5B	0.01	0	0.19	5B	15.74	15.5	14.39
6C	0	0	0.12	6C	9.23	9.15	8.87
7D	0	0	0.1	7D	6.3	6.24	5.93
a4	0	0	0.11	a4	5.22	5.17	5.04
c3	0	0	0.11	c3	5.24	5.19	5.05
c4	0	0	0.16	c4	6.13	6.05	5.74
2D	0	0	0.11	2D	5.22	5.17	5.04
6E	0	0	0.11	6E	5.34	5.29	5.15
All other	0	0	0.11	All other	5.22	5.17	5.03

4.2. Players mixed strategies payoffs

The performance of the miniature oil supply model is considered under three fuel pricing scenarios, and two instances of disruption severity. The payoffs are broken down in terms of operational expenses (OpEx) and SO_x cost (which is further broken down to SO_x emissions cost within and out of ECAs). For the environmental policy and network resilience analysis undertaken, the payoffs of the conductor strategies that involve ECAs are evaluated as the sum of OpEx and SO_x emissions cost within ECAs. For conductor strategy 3 (that doesn't involve ECAs), it is considered to be in the discretion of the conductor to account or not for the coastal SO_x, and therefore two payoff values are obtained, one including SO_x and one only considering OpEx.

The players optimal strategies to the games for all fuel pricing options and disruption intensity levels are summarized in Table 8. The saddle points for the low intensity games (where Nature is assumed to assign equal probability to all disruption strategies) are obtained by solving the residual linear optimization that chooses the optimal conductor strategy that minimizes Nature's payoff. The optimal conductor strategy is to avoid the adoption of ECAs for all fuel pricing scenarios, except for FP3, where the SO_x cost is higher than the OpEx savings when no ECAs is imposed. For low fuel pricing, the conductor is better off adopting the enhanced ECAs with optimal vessel speed strategy (2: ECA_opt).

Table 8: Optimal strategies for both players (Conductor, Nature/ Disruptor)

3: No ECA Payoff …	Intensity	FP1	FP2	FP3
… SO_x Excluded	Nature	(100% 3, N/A)	(100% 3, N/A)	(100% 3, N/A)
	Attacker	(100% 3, 100% 5B)	(100% 3, 100% 5B)	(100% 3, 100% 5B)
… SO_x Included	Nature	(100% 3, N/A)	(100% 3, N/A)	(100% 2, N/A)
	Attacker	(100% 3, 100% 5B)	(100% 3, 100% 5B)	(100% 3, 100% 5B)

The saddle points for the high intensity games (where the disruptor is assumed to maximize his payoff) are solved by elimination by dominance, as the disruption of arc 5B is found to always yield the highest payoff to the attacker. The optimal strategy for the conductor is always to avoid the adoption of ECAs.

Considering the optimal strategies for both players, the expected payoffs for the conductor are illustrated in Table 9. The baseline cost for operating the supply chain is considered to be the enhanced ECA strategy with no disruptions, 12 knots slow steaming, and optimized vessel speed (using LVOM).

Table 9: Expected conductor payoffs and cost (shown in parenthesis) considering both player strategies

3: No ECA Payoff …	Intensity	FP1	FP2	FP3
…SO_x Excluded	Nature	-0.43 (5.60)	-0.76 (8.79)	-0.25 (2.88)
	Attacker	-9.03 (14.20)	-14.55 (22.58)	-4.18 (6.81)
…SO_x Included	Nature	-0.55 (5.72)	-0.88 (8.91)	-0.35 (2.98)
	Attacker	-9.22 (14.39)	-14.74 (22.77)	-4.37 (7.00)
Baseline		5.17	8.03	2.63

4.3. Environmental policy and price sensitivity

By considering three fuel pricing scenarios and observing that the optimal strategy for the conductor changes for the lower priced one (FP3), it is found that the conductor's choice to consider ECAs or not is a function of fuel and SO_x price. Although the proposed model does not account for the profits of operating the supply chain, the cost minimization considered advocates against the adoption of ECAs. This is because the operational cost added exceeds the environmental benefit achieved. This is captured in Figure 6, when squares (that represent the network cost for "ECA enhanced" strategy) are compared to triangles (that represent the No ECA including SO_x cost). The scatter plot of Figure 6 presents the network cost for all strategy i and j combinations against universal fleet speed for FP3. The exponential trendlines of Figure 6 illustrate that for higher universal fleet speed, the two strategy payoffs diverge further.

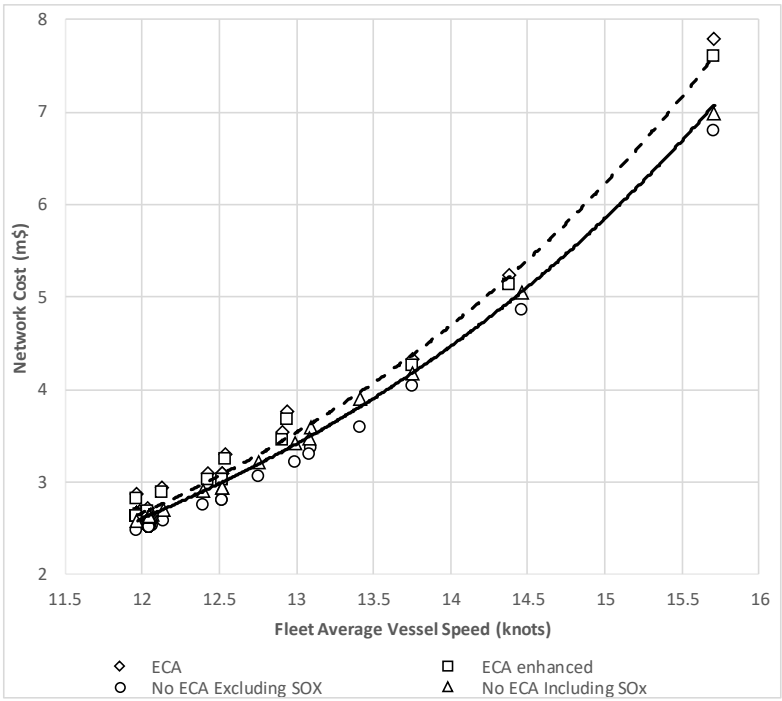

Figure 6: Total OpEx and $\boldsymbol{SO_x}$ cost (m$) for FP3 for all strategy $\boldsymbol{i}$ and $\boldsymbol{j}$ combinations shown as a function of universal fleet speed required (knots)

A sensitivity analysis is conducted to examine for which SO_x prices, the "ECA enhanced" strategy becomes optimal for various disruption scenarios. Table 10 illustrates the adjustment in SO_x price required for each fuel price scenario considered.

Table 10: Average $\boldsymbol{SO_x}$ price adjustment required for "ECA enhanced" strategy to become optimal

Fuel Price Scenario	SO_x price adjustment ($/kg)		
	Average	1st highest disruption	2nd highest disruption
FP1	8.71	43.24	22.09
FP2	13.89	59.84	31.72
FP3	-3.48	22.45	3.18

In all game scenarios examined, the attacker chooses the disruption of arc "5B" (indicated in the top right corner of Figure 6), and the SO_x price increase required to make "ECA enhanced" optimal is 22.45$ as shown in Table 10. This figure is substantially higher than the price increase required for the second highest disruption, which is a 3.18$ SO_x when arc "c4" is disrupted. It can therefore be argued that instead of setting a SO_x price high enough to make "ECA enhanced" optimal for all disruptions, an SO_x price that covers most disruptions is set, while the "No ECA" strategy is adopted for more severe disruptions.

5. Conclusions

5.1. Concluding remarks

In recent years the introduction of new environmental and security regulations has influenced the way supply chains are operated globally. Maritime operators have been in search of optimal strategies to improve performance while complying with regulatory requirements in an increasingly complex regulatory framework. This research establishes a link between

environmental and network resilience performance for maritime supply chains, and provides a methodological framework to analyze the impact of various abatement options, regulatory and pricing strategies. The proposed methodology, utilizes minimum cost flow assignment and link speed optimization to establish operational performance and SO_x emissions cost, and a game theoretic model to compare various operational and environmental strategies in terms of network resilience.

A case study is undertaken on a miniature model of the oil supply chain. The analysis confirms that ECA policy increases the cost to operate a supply chain. In the case study examined, using recent pricing it was found that ECA policy is not implemented effectively, as it is not an optimal choice. To become one SO_x emissions reduction should be valued higher. By repeating the analysis for various fuel pricing options, it was observed that it is in the benefit of the operator to not comply unless fuel pricing is very low. The lack of a link between SO_x price and fuel pricing, was determined to be the cause of this behavior, which can be overcome by making SO_x price a function of fuel pricing. A sensitivity analysis undertaken on SO_x pricing indicated price adjustments required for making ECA policy effective.

The disruptor-conductor game indicated that a malevolent player can yield an increase to the operational cost of the network up to 280% (under the examined conditions). For all extreme disruptions, the conductor's optimal strategy is found to be to avoid the implementation of ECAs regulation. The amount by which operational cost outweighs SO_x emission savings value is found to increase exponentially with increasing disruption severity (shown as a function of fleet speed in Figure 6).

The proposed methodological framework can be used both for decision-making and performance improvement purposes. There are growing concerns on the appropriateness of ECAs as an environmental strategy due to potential modal shifts, increased transportation costs, and the lack of fairness compared to ship and port operators that are unaffected by the low-sulphur requirements. The proposed methodology should be used by policy makers to simulate the effects of suggested policies to the full network when considering alternative emissions abatement procedures. The case study has shown the practical applicability of the proposed methodology capturing how environmental legislation in one area may have significant indirect consequences to other areas and the global network.

5.2. Limitations and future work

The proposed methodology better equips policy makers to manage environmental and resilience legislation, and supply chain operators who consistently seek to minimise operational costs, also minimize their exposure to costly supply chain disruptions. The incapacity of the proposed flow assignment methodology to account for various vessel speeds, and the sub-optimality of the heuristic are recognized limitations of the model and further work is proposed to improve analytic accuracy and detail. It would also be interesting to examine the same problem in a liner shipping network, bearing in mind that certain things would need to be changed. For example, instead of using tonnage to define fleet capacity, one should look at the TEU capacity of the global liner shipping fleet. Further work is also proposed in determining an appropriate SO_x pricing strategy using real world data on supply chain operations and establish ways to identify which disruptions should trigger an ECA regulations short-term cut-off. It should be noted that the effects of SECA on sailing speed optimization will be more limited once the global limit is reduced to 0,5%. However, there may be additional

local environmental regulations coming into place in the near future that will have similar effects on maritime networks.

6. Appendix

Table 11: SO_x emissions cost and total payoff for FP2 scenario for all strategy ***i*** and ***j*** combinations

SO_x Payoff within ECA (m$)				Total Payoff (m$)			
Disruptor strategy ***j***	Conductor strategy ***i***			Disruptor strategy ***j***	Conductor strategy ***i***		
	1: ECA	2: ECA_opt	3: ECA		1: ECA	2: ECA_opt	3: ECA
None	0	0	0.11	**None**	8.08	8.03	7.83
a1	0	0	0.14	a1	9.64	9.56	9.23
a2	0	0	0.11	a2	8.28	8.23	8.02
a7	0	0	0.15	a7	9.93	9.86	9.45
b4	0	0	0.11	b4	8.11	8.06	7.86
b5	0.01	0	0.17	b5	11.37	11.26	10.55
c6	0	0	0.14	c6	13.74	13.66	13.32
1A	0	0	0.14	1A	9.64	9.56	9.23
2A	0	0	0.11	2A	8.27	8.22	8.02
5B	0.01	0	0.19	5B	24.54	24.28	22.77
6C	0	0	0.12	6C	14.37	14.28	13.89
7D	0	0	0.1	7D	9.7	9.64	9.21
c3	0	0	0.11	c3	8.11	8.06	7.85
c4	0	0	0.16	c4	9.5	9.42	8.96
2D	0	0	0.11	2D	8.09	8.03	7.83
6E	0	0	0.11	6E	8.27	8.22	8.01
All other	0	0	0.11	All other	8.08	8.03	7.83

Table 12: SO_x emissions cost and total payoff for FP3 scenario for all strategy ***i*** and ***j*** combinations

SO_x Payoff within ECA (m$)				Total Payoff (m$)			
Disruptor strategy ***j***	Conductor strategy ***i***			Disruptor strategy ***j***	Conductor strategy ***i***		
	1: ECA	2: ECA_opt	3: ECA		1: ECA	2: ECA_opt	3: ECA
None	0	0	0.12	**None**	2.67	2.63	2.64
a1	0	0	0.14	a1	3.1	3.04	2.95
a2	0	0	0.22	a2	2.87	2.82	3.59
a7	0.01	0	0.21	a7	3.55	3.46	3.43
b4	0	0	0.12	b4	2.69	2.65	2.65
b5	0.01	0	0.3	b5	3.77	3.68	3.9
c6	0	0	0.14	c6	4.33	4.27	4.18
1A	0	0	0.14	1A	3.1	3.04	2.95
2A	0	0	0.15	2A	2.94	2.9	3.22
5B	0.01	0	0.19	5B	7.81	7.61	7
6C	0.01	0	0.18	6C	5.24	5.14	5.05
7D	0	0	0.18	7D	3.31	3.26	3.48
c3	0	0	0.12	c3	2.69	2.65	2.65
c4	0	0	0.16	c4	3.1	3.04	2.92
6B	0	0	0.11	6B	2.67	2.63	2.59
6E	0	0	0.12	6E	2.73	2.69	2.7
All other	0	0	0.12	All other	2.67	2.63	2.64

7. References

1. Achurra-Gonzalez, P. E., Novati, M., Foulser-Piggott, R., Graham, D.J., Bowman, G., Bell, M.G.H., and Angeloudis, P. (2016) Modelling the impact of liner shipping network perturbations on container cargo routing: Southeast Asia to Europe application. *Accident. Analysis & Prevention*, no. 4134.
2. Acciaro, M., and Serra, P. (2013) Maritime supply chain security: A critical review. IFSPA 2013: Trade, Supply Chain Activities and Transport: Contemporary Logistics and Maritime Issues, Hong Kong.

3. Angeloudis, P., Bichou, K., Bell, M.G.H. and Fisk, D. (2007) Security and reliability of the liner container-shipping network: analysis of robustness using a complex network framework. *Risk Management in Port Operations, Logistics and Supply Chain Security*, pp. 95–106.
4. Benford, H. (1981) A simple approach to fleet deployment. *Maritime Policy & Management*, 8, (4) 223–228.
5. Berle, O., Asbjornslett, B.E. and J. Rice (2011) Formal vulnerability assessment of maritime transportation system. *Reliability Engineering and System Safety*, 96, 696-705.
6. Bichou, K. (2008) Security and Risk-Based Models in Shipping and Ports: Review and Critical Analysis. Joint Transport Research Centre, Discussion Paper N. 2008-20, December 2008.
7. California Air Resources Board (CARB) (2012) Marine Notice 2012-1: Advisory to owners or operators of ocean-going vessels or ships visiting California ports. Available at: http://www.arb.ca.gov/ports/marinevess/ documents/marinenote2012_1.pdf, accessed April 2015.
8. Cariou, P. (2011) Is slow steaming a sustainable means of reducing CO 2 emissions from container shipping? *Transportation Research Part D: Transport and Environment*, 16(3), 260-264.
9. Corbett, J. J., Wang, H., and Winebrake, J.J. (2009) The effectiveness and costs of speed reductions on emissions from international shipping. *Transportation Research Part D: Transport and Environment*, 14, (8) 593-598.
10. Cox, A., Prager, F. and Rose, A. (2011) Transportation security and the role of resilience: A foundation for operational metrics. *Transport Policy*, no. 18, pp. 307-317.
11. Cullinane, K., and, Bergqvist, R. (2014) Emission control areas and their impact on maritime transport. *Transportation Research Part D: Transport and Environment*, 28, 1-5.
12. Doudnikoff, M., and, Lacoste, R. (2014) Effect of a speed reduction of containerships in response to higher energy costs in Sulphur Emission Control Areas. *Transportation Research Part D: Transport and Environment*, 28, 51-61.
13. Ducruet, C., Lee, S.-W.**,** and Ng, A.K.Y. (2010) Centrality and vulnerability in liner shipping networks: revisiting the Northeast Asian port hierarchy," *Maritime Policy & Management*, vol. 37, no. 1, pp. 17–36.
14. Ducruet, C., and Zaidi, F. (2012) Maritime constellations: a complex network approach to shipping and ports. *Maritime Policy & Managment*, vol. 39, no. 2, pp. 151–168.
15. Energy Information Administration (2010) Petroleum marketing annual 2009. Office of Oil and Gas, US Department of Energy, Washington DC.
16. Eyring, V., Köhler, H. W., Van Aardenne, J., & Lauer, A. (2005). Emissions from international shipping: 1. The last 50 years. Journal of Geophysical Research: Atmospheres, 110(D17).
17. Fagerholt, K., and Psaraftis, H.N. (2015). On two speed optimization problems for ships that sail in and out of emission control areas. *Transportation Research Part D: Transport and Environment*, 39, 56-64.
18. Golias, M., Portal, I., Konur, D., Kaisar, E., and Kolomvos, G. (2014) Robust berth scheduling at marine container terminals via hierarchical optimization. *Computers & Operations Research*, 41, 412-422.
19. Hendricks, K.B., Singhal, V.R., 2005. An empirical analysis of the effect of supply chain disruptions on long-run stock price performance and equity risk of the firm. Prod. Oper. Manage. 14 (1), 35–52.
20. International Energy Agency (IEA) (2007) Energy Security and Climate Policy: Assessing Interactions. Paris, France.
21. International Energy Agency (IEA) (2014) Energy Supply Security 2014. Paris, France.
22. Khersonsky, Y., Islam, M. and Peterson, K. (2007) Challenges of Connecting Shipboard Marine Systems to Medium Voltage Shoreside Electrical Power. Industry Applications, IEEE 43, (3) 838 –844.
23. Kim, Y., Chen, YS. And K. Linderman (2015) Supply network distribution and resilience: A network structural perspective. *Journal of Operations Management*, 33-34, 43-59.
24. Lai, K.-h., Wong, C.W.Y. and Jasmine, S.L.L (2015) Sharing environmental management information with supply chain partners and the performance contingencies on environmental munificence. *International Journal of Production Economics, 164, 445-453.*
25. Levalle, R. R. & Nof, S. Y. (2015). Resilience by teaming in supply network formation and re-configuration. International Journal of Production Economics, 160, 80-93.
26. Lhomme, S. (2015) Vulnerability and resilience of ports and maritime networks to cascading failures and targeted attacks. *Maritime networks: spatial structures and time dynamics*, by C. Ducruet. Ed: Routledge, 2015.
27. Lloyd's MIU (2008) Lloyd's MIU Handbook of Maritime Security.
28. Maloni, M., Paul, J.A. and, Gligor, D.M. (2013) Slow steaming impacts on ocean carriers and shippers. *Maritime Economics & Logistics* 15, (2) 151–171.
29. MAN Diesel and Turbo (2012) Propulsion of VLCC. Denmark.
30. MAN Diesel and Turbo (2014) Electronically controlled two-stroke Engines with Camshaft controlled exhaust valves. Denmark.
31. Oil and Gas Journal (2011) Oil and Gas Journal Databook 2010.
32. Ouyang, M., Zhao, L., Hong, L., and Pan, Z. (2014). Comparisons of complex network based models and real train flow model to analyze Chinese railway vulnerability. *Reliability Engineering & Systems Safety*, vol. 123, pp. 38–46.
33. Perea, S.S., Bell, M.G.H. and M.C. Bliemer (2015) Modelling supply chains as complex networks for investigating resilience: an improved methodological network. *Australian Transport Research Forum(ATRF), 3th*.
34. Prousalidis, J., Hatzilau, I. K., Michalopoulos, P., Pavlou, I., and Muthumuni, D. (2005) Studying ship electric energy systems with shaft generator. In Electric Ship Technologies Symposium, 2005 IEEE, 156-162.
35. Psaraftis, H. N. and, Kontovas, C.A. (2013) Speed models for energy-efficient maritime transportation: A taxonomy and survey. *Transportation Research Part C: Emerging Technologies*, 26, 331-351.
36. Qiao, W., Lu, Y., Xiong, C. and Haghani, A. (2014) A game theory approach for the measurement of transport network vulnerability from the system prospective. *Transportmetrica B: Transport Dynamics*, vol. 2, no. 3, pp. 188–202
37. Reggiani, A. (2013) Network resilience for transport security: Some methodological considerations. *Transport Policy*, no. 28, pp.63-68.
38. Ricardo-AEA (2014). *Update of the Handbook on External Costs of Transport.* Report for the European Commission DG MOVE, London.
39. Ronen, D. (1982) The effect of oil price on the optimal speed of ships. *Journal of the Operational Research Society*, 1035-1040.
40. Sheffi, Y. and J.B. Rice (2005) A supply chain view of the resilient enterprise. *MIT Sloan Management Review*, 47, 1, 41-48.
41. Sullivan, J. L., Novak, D. C., Aultman-Hall, L. and Scott, D. M. (2010) Identifying critical road segments and measuring system-wide robustness in transportation networks with isolating links: A link-based capacity reduction approach. *Transportation Research Part A: Policy and Practice*, vol. 44, no. 5, pp. 323–336.
42. Supply Chain Digest (2006) The 11 greatest supply chain disasters.
43. Tichavska, M., Tovar, B., Gritsenko, D., Johansson, L. and J.P. Jalkanen (2017) Air emissions from ships in port: Does regulation make a difference?. *Transport Policy* [In press] Accessed online.

44. UNCTAD (2017) Review of Maritime Transport 2017.
45. Vilko, J. and Hallikas, J. (2012) Risk assessment in multimodal supply chains. *International Journal of Production Economics*, 140, 586-595.
46. Wasserman, S., Faust, K., 1994. Social Network Analysis: Methods and Applications.Cambridge University Press, New York, NY.
47. World Economic Forum (2016) The Global Risks Report 2016.
48. World Trade Organization (2016) World Trade Statistical Review 2016.
49. Zavitsas, K. (2011) Vulnerability of the Petroleum Supply Chain. PhD thesis, London.
50. Zis, T., & Psaraftis, H. N. (2018). Operational measures to mitigate and reverse the potential modal shifts due to environmental legislation. Maritime Policy & Management, 1-16.
51. Zis, T., & Psaraftis, H. N. (2017). The implications of the new sulphur limits on the European Ro-Ro sector. *Transportation Research Part D: Transport and Environment*, *52*, 185-201.
52. Zis, T., North, R. J., Angeloudis, P., Ochieng, W. Y., and Bell, M.G.H. (2014). Evaluation of cold ironing and speed reduction policies to reduce ship emissions near and at ports. *Maritime Economics & Logistics*, 16(4), 371-398.
53. Zis, T., North, R. J., Angeloudis, P., Ochieng, W. Y., and Bell, M.G.H. (2015). The Environmental Balance of Shipping Emissions Reduction Strategies. In *Transportation Research Record: Journal of the Transportation Research Board*, No. 2479, pp. 25–33